

## Reaction $^{48}\text{Ca}(p, n)^{48}\text{Sc}$ from $E_p = 1.885$ to $5.1$ MeV

GULZAR SINGH\*, S KAILAS, S SAINI, A CHATTERJEE,  
M BALAKRISHNAN and M K MEHTA

Nuclear Physics Division, Bhabha Atomic Research Centre, Bombay 400 085.

\*Cyclotron Laboratory, Panjab University, Chandigarh 160 014, India

MS received 23 August 1982

**Abstract.** The total  $(p, n)$  reaction cross section for  $^{48}\text{Ca}$  has been measured as a function of proton energy in the energy range 1.885 to 5.100 MeV with an overall resolution of  $\sim 2$  keV and in  $\sim 5$  keV energy steps. The fluctuations in fine resolution data have been analysed to determine the average coherence width  $\langle \Gamma \rangle$ . The excitation function averaged over large energy intervals has been analyzed in terms of the optical model. The isobaric analogue resonances at  $E_p \sim 1.95$  and 4 MeV have been shape-analyzed to extract the proton partial width and the spectroscopic factor  $S_n$ . A comparison of the gross structures observed in  $\sim 55$  keV averaged excitation function with the predictions of Izumo's partial equilibrium model has also been made.

**Keywords.**  $(p, n)$  reaction;  $^{48}\text{Ca}$  target; extracted  $\langle \Gamma \rangle$ ; isobaric analogue resonance parameters; optical model parameters; intermediate width structures.

### 1. Introduction

In continuation of our programme of studies of  $(p, n)$  reactions below the Coulomb barrier on medium weight nuclides (Kailas *et al* 1975b; Mehta *et al* 1977; Viyogi *et al* 1978; Kailas *et al* 1979) through measurement of excitation functions, the total  $(p, n)$  cross-section for the reaction  $^{48}\text{Ca}(p, n)^{48}\text{Sc}$  has been measured in the bombarding energy range from  $\sim 1.885$  to  $5.100$  MeV with fine resolution. The main aims of this work are to determine the optical model parameters for the target plus proton system at these low energies, to extract the coherence width from a fluctuation analysis of the fine structure data and to study in detail the isobaric analogue resonances (IAR) observed. The  $^{48}\text{Ca} + p$  system at these energies has been studied by various workers with some of the motivations discussed above. El-Nadi *et al* (1965) have determined  $\sim 90$  levels in  $^{48}\text{Sc}$  from  $\sim 10.6$  to  $11.9$  MeV excitation through  $^{48}\text{Ca}(p, n\gamma)$  reaction for  $E_p \sim 1 \sim 2.5$  MeV. McMurray *et al* (1967) have determined the average coherence width to be  $\sim 9$  keV at about 15 MeV excitation energy in  $^{48}\text{Sc}$  from a fluctuation analysis of differential cross-sections for the reaction  $^{48}\text{Ca}(p, n)^{48}\text{Sc}$  for various neutron groups in the proton energy from 4 to 5.6 MeV with an overall resolution of  $\sim 8$  keV. From a measurement of  $^{48}\text{Ca}(p, \gamma)$ ,  $^{48}\text{Ca}(p, n)$  reaction cross-sections for  $E_p \sim 0.57$  to  $2.67$  MeV, Zyskind *et al* (1979) have shown that the excitation function behaviour can be well explained by a Hauser-Feshbach calculation. They have also determined thermonuclear reaction rates from  $\sigma_{p, n}$ ,  $\sigma_{p, \gamma}$  measurements. The IARs in  $^{48}\text{Sc}$  have been mainly studied through  $(p, p)$  (Jones *et al* 1966; Vingiani *et al* 1968;

Gaarde *et al* 1972) and  $(p, n \gamma)$  (Wilhjelm *et al* 1969, Chilosi *et al* 1968; Gaarde *et al* 1972) reactions on  $^{48}\text{Ca}$ . But for Jones *et al* (1966), the others have concentrated only on the analogue of the ground state of  $^{48}\text{Ca}$ . Sekharan and Mehta (1969) have also studied the IAR at  $E_p \sim 1.95$  MeV through  $^{48}\text{Ca}(p, n)$  reaction. Even though the results of these various measurements in general agree with each other, there are still differences and certain ambiguities in the extraction of IAR parameters.

With a view to extend the  $(p, n)$  cross-section measurement to a larger energy range, to confirm and improve the accuracy wherever possible of the results obtained by various workers and with the broad motivations mentioned earlier we have carried out a detailed measurement of the total  $(p, n)$  cross-section for the reaction  $^{48}\text{Ca}(p, n)$ .

The paper is divided into various sections. In §2, the experimental technique and the results are discussed. Section 3 deals with the analysis of the data in terms of the optical model, statistical model and Robson-Johnson procedure. The general conclusions are summarized in §4.

## 2. Experimental procedure and results

The total  $(p, n)$  cross-section for the reaction  $^{48}\text{Ca}(p, n)^{48}\text{Sc}$  has been measured utilizing a  $4\pi$  neutron counter and the thin target technique. Details of the experimental technique are given elsewhere (Kailas *et al* 1975b). The enriched  $^{48}\text{Ca}$  target in the form of  $\text{CaCO}_3$  (84.42%  $^{48}\text{Ca}$ , 14.55%  $^{40}\text{Ca}$ , 0.123%  $^{42}\text{Ca}$ , 0.042%  $^{43}\text{Ca}$  and 0.66%  $^{44}\text{Ca}$ ) deposited on a thick ( $\sim 2$  mm) Ta backing was obtained from AERE Harwell, UK. The target thickness as determined from the low energy alpha backscattering technique (Kailas *et al* 1975b) was about 1 keV for 1.5 MeV protons. The overall energy resolution, including the beam energy spread, was better than 2 keV.

The excitation function was measured in 5 keV steps from  $E_p \sim 1.885$  MeV to  $\sim 5.1$  MeV proton energy and is displayed in figures 1 and 2. The IARs expected at  $E_p \sim 1.95$  MeV and  $\sim 4$  MeV are prominently seen in the excitation function.

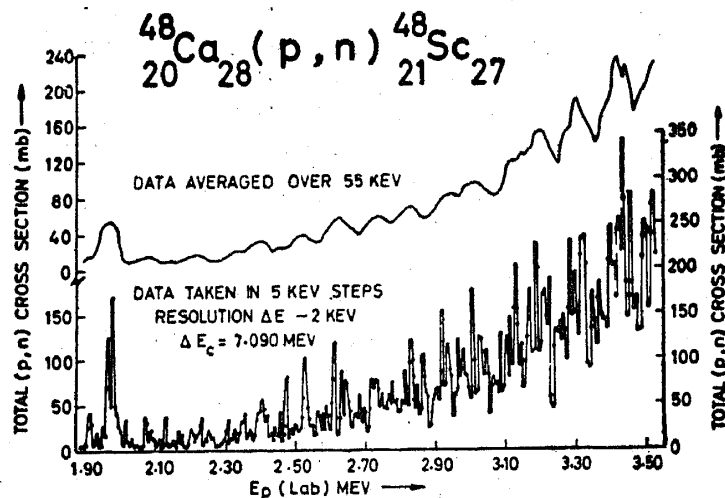


Figure 1. Excitation function for the  $^{48}\text{Ca}(p, n)^{48}\text{Sc}$  reaction from  $E_p = 1.885$  to 3.530 MeV.

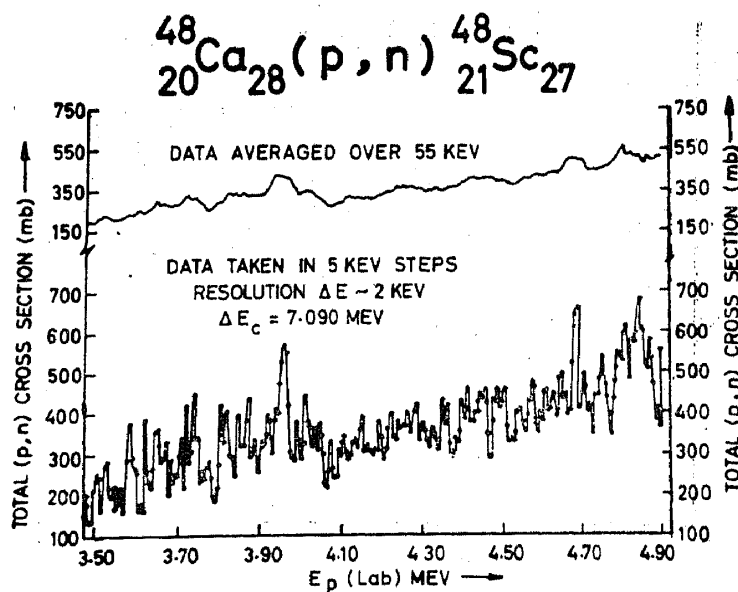


Figure 2. Excitation function for the  $^{48}\text{Ca}(p, n)^{48}\text{Sc}$  reaction from  $E_p = 3.470$  to  $5.10$  MeV.

But for these, the excitation function is marked by fluctuations. In order to determine better the shape of the strong IAR around  $E_p \sim 1.95$  MeV, the excitation function was remeasured in that energy region with  $0.6$  keV energy steps (Sckharan and Mehta, 1969). The absolute error in  $\sigma_{p,n}$  measurement is estimated to be  $\sim \pm 15\%$ . The error in the cross-section estimate due to the presence of the other Ca isotopes as well as  $^{13}\text{C}$  and  $^{17,18}\text{O}$  is expected to be negligible because of their lower abundance and/or larger negative  $Q_{p,n}$  values.

### 3. Analysis

#### 3.1 Optical model analysis

For a compound nuclear process the reaction cross-section is given by the Hauser-Feshbach (HF) formula based on the statistical model (Hauser and Feshbach 1952) and when level width fluctuations are taken into account the cross-section is given by Moldauer's modified expression (Moldauer 1964). At subcoulomb energies the neutron channel is the dominant reaction mode, and it is justified to assume  $\sigma_{p,n} \simeq \sigma_{\text{abs}}$ . This being the case it may be possible to fit the (p, n) data with a simple optical model calculation of  $\sigma_{\text{abs}}$ . In order to carry out this type of analysis, the fine structure data were averaged over an energy interval of  $\sim 115$  keV and the resultant smooth excitation function was fitted using the optical model. The calculations were performed using the optical model code OMOGLOB (Viyogi and Ganguly 1976). Besides the imaginary potential parameters  $W$  (depth) and  $a_I$  (diffuseness) which are the most sensitive to  $\sigma_{\text{abs}}$  calculation, the real potential depth  $V_{oR}$  was also varied to fit the (p, n) data. The other parameters were kept fixed at the global values given by Kailas *et al* (Kailas *et al* 1975a). The optical model fit to the data is shown in figure 3. The best fit parameters are listed in table 1.

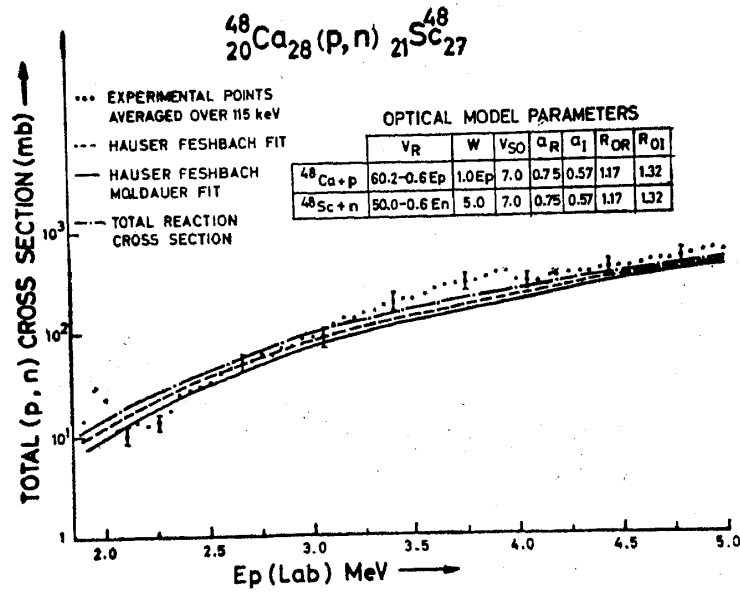


Figure 3. Optical model, HF and HFM fits to the energy averaged excitation function for the reaction  ${}^{48}\text{Ca}(p, n)$ . The structures observed around  $E_p = 2$  and 4 MeV are due to isobaric analogue resonances.

Table 1. List of the optical model parameters.

A.  ${}^{48}\text{Ca} + p$  system

Real potential

$V_{OR}$ (MeV)	$V_{sym}$ (MeV)	$V_{ER}$ (MeV)	$R_{OR}$ (fm)	$a_R$ (fm)	$R_{oc}$ (fm)
54	24	-0.6	1.17	0.75	1.20

Imaginary potential

$W$ (MeV)	$R_{OI}$ (fm)	$a_I$ (fm)
$1.0 E_p$	1.32	0.57

B.  ${}^{48}\text{Sc} + n$  system

Real potential

$$V_R = 50 - 0.6 E_n \quad R_{OR} = 1.17 \quad a_R = 0.75$$

(MeV)                      (fm)                      (fm)

Imaginary potential

$$W = 5 \quad R_{OI} = 1.32 \quad a_I = 0.57$$

(MeV)                      (fm)                      (fm)

For  ${}^{48}\text{Ca} + n$  system. (bound state calculation),

$$R_{OR} = 1.17 \quad a_R = 0.75$$

(fm)                      (fm)

$$V_{SO} = 7 \text{ MeV}; \quad R_{SO} = 1.17 \text{ fm}; \quad a_{SO} = 0.75 \text{ fm}$$

Note:

$$V(r) = -V_R f_R(r) + i4a_I W \frac{d}{dr} f_I(r) + V_c + 2V_{SO} \frac{1}{r} \frac{d}{dr} f_{SO}(r) L \cdot \sigma$$

where

$$f_x(r) = [1 + \exp \{(r - R_{ox})/a_x\}]^{-1}$$

$$V_R = V_{OR} + V_{sym} \frac{N-Z}{A} + 0.4 \frac{Z}{A^{1/3}} + V_{ER} E_p$$

It should be noted that the gross structures around the IARs at  $E_p \sim 1.95$  and 4 MeV cannot be explained by the smooth behaviour of  $\sigma_{\text{abs}}$  predicted by the optical model. In general (figure 3) one finds that the optical model somewhat overpredicts  $\sigma$  below  $E_p \sim 3$  MeV and the trend is reversed for energies above this. In order to understand better this feature a more involved HF and HFM calculations were carried out considering only the  $p$  and  $n$  decay channels, utilizing the known level schemes of  $^{48}\text{Sc}$ ,  $^{48}\text{Ca}$  (Gove and Wapstra 1972) and the  $p$  and  $n$  optical model parameters (table 1). The computer code HAFEC (Kailas *et al* 1976) was employed to compute the cross-section. The HF and HFM fits are shown in figure 3. It can be seen from the figure that the quality of fit to the data is more impressive for  $E_p$  up to 3 MeV. This clearly brings out the importance of HF and HFM calculations which take into account the level properties of the target and the residual nuclei. From this analysis it is clear in the present case that HF and HFM calculations will be more appropriate at lower energies than a simple optical model calculation of  $\sigma_{\text{abs}}$ . A general comment about the small misfit at the high energy region is that it is possible to improve the quality of fit by better tuning of the  $p$  and  $n$  optical model parameters and the inclusion of a more appropriate level density formula at higher excitation region for the residual nucleus  $^{48}\text{Sc}$ , instead of the discrete level scheme we have used in the present analysis.

### 3.2 Fluctuation analysis

As mentioned earlier, the striking feature of the data is the observation of a large number of fine structures (figures 1 and 2) which could be identified with Ericson fluctuations as discussed below. Before a full fledged fluctuation analysis is carried out, it is desirable to understand some of the features of these fine structures. It is found that the structures are having widths  $\Gamma \sim 5-10$  keV. Their average spacing works out to  $D \sim 10-15$  keV. Hence we get for  $\Gamma/D$  a value of the order of one. The average level spacing  $D$  for the levels with  $J^\pi = \frac{1}{2}^\pm, \frac{3}{2}^\pm, \frac{5}{2}^\pm$  likely to be populated in the compound nucleus  $^{49}\text{Sc}$  at the excitation energy,  $E_x \sim 13$  MeV works out to 1 keV (Gilbert and Cameron 1965). This is very small compared to the observed level spacing of  $\sim 10-15$  keV. This indicates that the observed structures are not the individual states of the compound nucleus. Further, one can estimate  $\Gamma/D$  using the relation,

$$\Gamma/D = \sum_e T_c / 2\pi \quad (1)$$

where  $T_c$  are the transmission coefficients. Utilizing the proton and neutron transmission coefficients computed from the optical model discussed in §3.1 we estimate  $\Gamma/D \sim 6$ . This clearly establishes that we have overlapping structures in the excitation function. The conclusion regarding the statistical nature of the observed fluctuations is further justified by the observation of McMurray *et al* (1967) who from a study of  $^{48}\text{Ca}(p, n)$  reaction do not find presence of cross correlation between pairs of excitation function curves corresponding to different neutron groups. In view of these above mentioned features, we felt a detailed statistical analysis of the data will be in order. We have extracted the coherence width  $\langle \Gamma \rangle$  from the autocorrelation

and peak counting methods (Braga Marcazzan and Milazzo Colli 1970). The autocorrelation function is defined as

$$C(\epsilon) = \left( \frac{\Delta E}{E_2 - E_1} \right) \sum_{E=E_1}^{E_2} \left[ \frac{(\sigma(E) - \langle \sigma(E) \rangle_\delta) (\sigma(E + \epsilon) - \langle \sigma(E + \epsilon) \rangle_\delta)}{\langle \sigma(E) \rangle_\delta \langle \sigma(E + \epsilon) \rangle_\delta} \right] \quad (2)$$

$E_2$ ,  $E_1$  are the upper and lower limits of the bombarding energy,  $\sigma(E)$  is the cross-section at the bombarding energy  $E$ ,  $\Delta E$  is the energy step with which the excitation function is measured, the  $\langle \rangle_\delta$  indicates the average cross-section over an energy range  $\delta E$  and  $\epsilon$  is the energy increment equal to  $n \times \Delta E$  with  $n$  as an integer. In figure 4 we have plotted the  $C(0)$  as a function of the local averaging interval in order to help in deciding the appropriate  $\delta E$  value to be used in  $\Gamma$  evaluation. As discussed by Mehta *et al* (1966), to extract the coherence width from the correlation function the value of  $\delta E$  should be chosen from the flat portion of the curve of figure 4.

According to the fluctuation theory (Braga Marcazzan and Milazzo Colli 1970),  $C(\epsilon)$  is given by

$$C(\epsilon) = C(0) \frac{\Gamma^2}{\Gamma^2 + \epsilon^2} \quad (3)$$

In figure 5,  $C(\epsilon)$  values are plotted as a function of  $\epsilon$  for  $\delta E$  values 200, 220 and 240 keV which lie in the plateau region of figure 4. The solid lines are the Lorentzian curves given by expression (3) above. The Lorentzian shape is expected only for the very low values of  $\epsilon$  and for larger values of  $\epsilon$  one expects oscillations due to finite range of data used. So the fit to Lorentzian has been made only for the first few

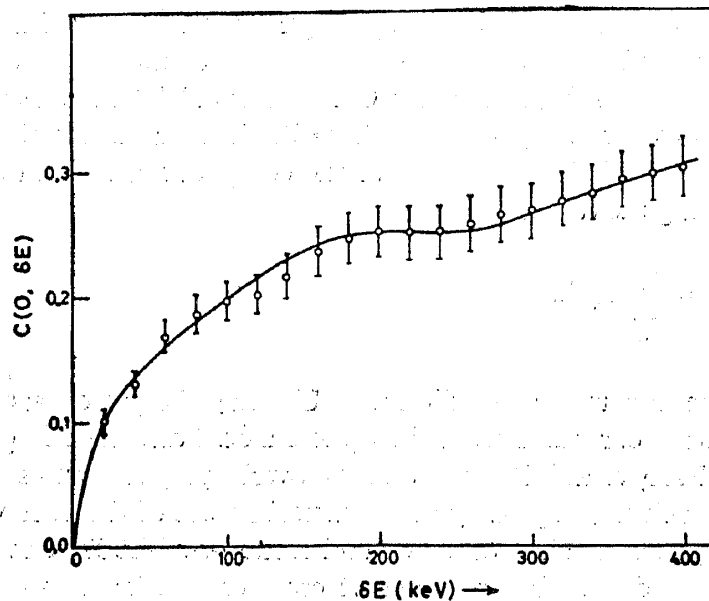


Figure 4. Selection of appropriate averaging energy interval  $\delta$  for  $\Gamma$  extraction. A plot of normalised variance  $C(0)$  versus averaging energy interval  $\delta$ . The errors indicated arise due to finite range of data (FRD) considered.

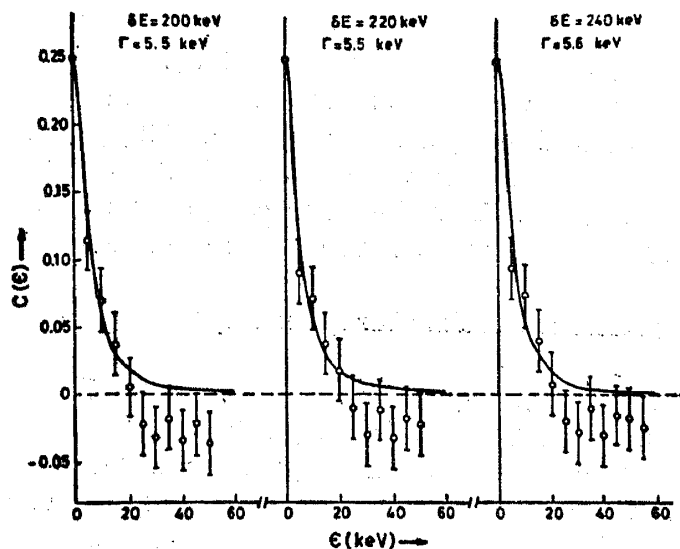


Figure 5. Fits of normalised auto-correlation function  $C(\epsilon)$  to the Lorentzian  $C(0) \Gamma^2/(\Gamma^2 + \epsilon^2)$  for specified values of  $\delta$ , for  $\delta = 200, 220, 240$  keV.

$\epsilon$  values and the best fit values of  $\Gamma$  are given in figure 5. The average  $\langle \Gamma \rangle$  extracted from this method is  $5.5 \pm 1.1$  keV. The error quoted is mainly due to the finite range of data considered here.

The  $\langle \Gamma \rangle$  has also been extracted following the counting of maxima method (Braga Marcazzan and Milazzo Colli 1970). The corrections due to energy resolution and step size were applied as discussed in the above reference. The  $\langle \Gamma \rangle$  works out to  $9.7 \pm 0.8$  keV. This we feel could be the upper limit and we cannot rule out the fact that some peaks have been missed in the counting process. The  $\langle \Gamma \rangle$  from the autocorrelation can be considered to be more reliable.

One of the applications of  $\langle \Gamma \rangle$  extracted is in the determination of the level density parameter  $a$ . Following Braga Marcazzan and Milazzo Colli (1970), we have

$$\sum_J (2J+1)^2 \left[ \frac{1}{4\pi^2 \langle \Gamma \rangle^2 \rho^2(E, J) + A_J^2} - \frac{1}{2A_J^2} \right] \times \sum_s \sum_l T_l^2 \sum_{s'} \sum_{l'} T_{l'}^2 = 0, \quad (4)$$

where  $A_J = \sum_c \ln \frac{1}{1 - T_c^2}$

$s$  ( $s'$ ) and  $l$  ( $l'$ ) stand for the spin and orbital angular momentum of the entrance (exit) channel.  $T$ 's are the transmission coefficients.  $c$  stands for possible decay channels for the compound nucleus level ( $J^\pi$ ) at energy  $E$ . Here the only unknown quantity is the level density  $\rho(E, J)$ .

In this calculation, we consider  $T$ 's only for  $J^\pi = \frac{1}{2}^\pm, \frac{3}{2}^\pm, \frac{5}{2}^\pm$ , the most probable values. We consider an average excitation of 13 MeV for the compound nucleus  $^{49}\text{Sc}$ . Using the known level schemes of  $^{48}\text{Ca}$  and  $^{48}\text{Sc}$  (Gove and Wapstra 1972) the  $p$  and  $n$  transmission coefficients computed as discussed in § 3.1 and  $\langle \Gamma \rangle$  as 5.5 keV, equation (3) was solved to extract  $\rho(E, J)$ . Using the level density expression of Gilbert and Cameron (1965) and the value for  $\rho(E, J)$  deduced above, we have extracted the parameter  $a$  to be  $4.2 \pm 0.3 \text{ MeV}^{-1}$ . This is somewhat lower compared to the value  $\sim 6$  obtained from the systematics of the level density parameter. This difference can perhaps be attributed to the specific structure effects of the residual nucleus considered here.

### 3.3 Isobaric analog resonances and nuclear spectroscopy

**3.3a General remarks and useful expressions.** Starting with the Coulomb displacement energy ( $\Delta E_c$ ) for  $^{49}\text{Ca}$  (parent) and  $^{49}\text{Sc}$  (analogue) pair as 7.09 MeV (Jänecke 1969) and the ground state neutron separation energy ( $S_n$ ) from  $^{49}\text{Ca}$  as 5.15 MeV (Gove and Wapstra 1972) we predict the analogue of the ground state of  $^{49}\text{Ca}$  to occur at  $E_p(\text{cm}) \sim 1.94 \text{ MeV}$ . Similarly the analogue of the first excited state ( $E_x = 2.03 \text{ MeV}$ ) should occur at  $E_p(\text{cm}) \approx 3.97 \text{ MeV}$ . Looking at the  $^{48}\text{Ca}(p, n)^{48}\text{Sc}$  excitation function displayed in figures 1 and 2 one notices prominent structures at  $E_p(\text{lab}) \sim 1.95$  and  $\sim 4 \text{ MeV}$  which could be identified with the IARs expected. As the IARs have a large number of fine structures, one way of analyzing the data will be to measure these structures with fine resolution ( $\Delta E \sim 200\text{--}400 \text{ eV}$ ) and shape analyze several individual structures. The other approach will be to smear these fine structures by energy averaging and then carry out the shape analysis of the resulting single gross structure. In the present work we have followed the latter procedure as the energy resolution is not adequate to follow the former approach. The fine structure data over the two resonances around  $E_p \sim 1.98$  and  $\sim 4 \text{ MeV}$  were averaged by Gaussian resolution functions with widths of 14 and 140 keV respectively to average out the fine structures retaining the shape details. These are displayed in figures 6 and 7.

**3.3b Extraction of  $\Delta$ ,  $\Gamma_A$ ,  $\Gamma_p$  and  $W$ .** These averaged resonance shapes were fitted using the familiar Robson-Johnson expression (Johnson *et al* 1968)

$$\sigma_{p, n} = \sigma_{p, n}^*(\text{bkg}) \left[ \frac{(E_A - E - \Delta)^2}{(E_A - E)^2 + \Gamma_A^2/4} - 1 \right] + \sigma_p(\text{bkg}) \quad (5)$$

where parameters  $E_A$ ,  $\Delta$  and  $\Gamma_A$  have the usual meaning (Johnson *et al* 1968). The quantity  $\sigma_{p, n}^*(\text{bkg}) = g^J \pi \lambda^2 T_{p, n}^*$  where  $T_{p, n}^*$  is the non-resonant transmission factor for the same partial wave that would exist if the resonance was absent was computed using the optical model parameters listed in table 1. We treated the off-resonance background cross-section  $\sigma_p(\text{bkg})$  as a variable quantity (Kailas *et al* 1979) with the form  $A + B(E - E_{\text{min}})$  where  $E_{\text{min}}$  = low energy of the IAR and  $A$  and  $B$  are adjustable constants. A nonlinear least squares computer program has been used to fit the IAR with expression (5) with  $E_A$ ,  $\Gamma_A$ ,  $\Delta$ ,  $A$  and  $B$  as parameters. In figures 6 and 7 the continuous lines for the IARs represent the best shape fit curves. In table 2 the final values of the parameters are listed.



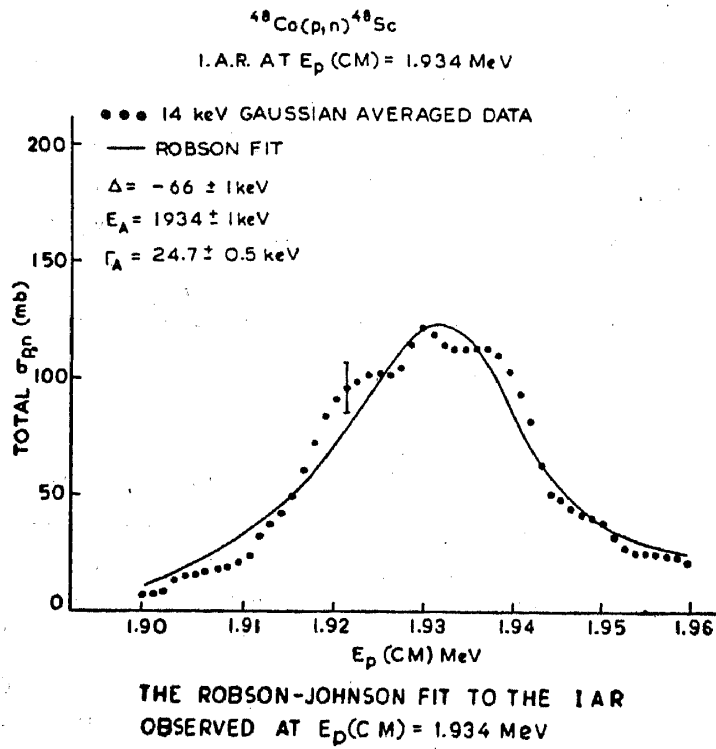


Figure 6. The Robson-Johnson fit to the IAR observed at  $E_p$  (CM) = 1.934 MeV.

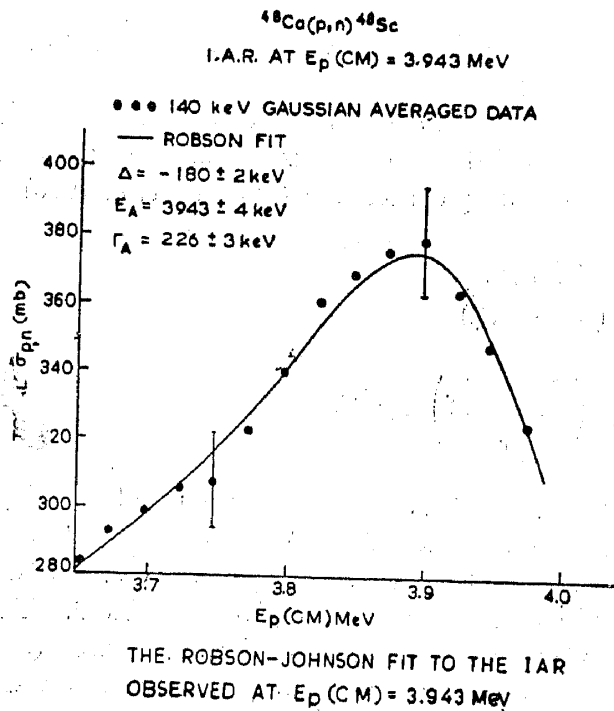


Figure 7. The Robson-Johnson fit to the IAR observed at  $E_p$  (CM) = 3.943 MeV.

Table 2. Parameters from Robson fits to analogue resonances.

Resonance parameters			Background parameters		
$E_A$ (keV)	$\Gamma_A$ (keV)	$\Delta$ (keV)	$\sigma_{p,n}^*$ (bkg) (mb)	$A$ (mb)	$B$ (mb/keV)
$1934 \pm 1$	$24.7 \pm 0.5$	$-66 \pm 1$	4.2	-17	0.64
$3943 \pm 4$	$226 \pm 3$	$-180 \pm 2$	35.6	237.5	0.204

Errors quoted have been obtained from the least squares fitting procedure.

Table 3. Results from IAR analysis

$E_A$ (keV)	$\Gamma_A$ keV	$\Gamma_p$ keV	$W$ ( $= \Gamma_n$ ) keV	$S_n$	Reference
Calculated <sup>(a)</sup>	Observed				
1940	1934	$24.7 \pm 0.5$	$1.97 \pm 0.10$	$13.8 \pm .7$	0.63 Present
	1940	$8.2 \pm 0.7$	$1.97 \pm 0.30$	$\sim 6.2$	0.64 Jones <i>et al</i> (1966)
		3.4	1.85	1.56	Wilhelm <i>et al</i> (1969)
			2.00	1.60	Gaarde <i>et al</i> (1972)
				1.03	Kashy <i>et al</i> (1965)
3970	3943	$226 \pm 3$	$151 \pm 2$	$52 \pm 1$	1.25 Present
	3860	200	136		1.24 Jones <i>et al</i> (1966)
					1.33 Kashy <i>et al</i> (1964)

<sup>(a)</sup> Calculated as discussed in § 3.3a.

Having extracted the  $\Delta$ -values for the two resonances, the proton partial width  $\Gamma_p$  and the spreading width  $W$  have been determined in the manner as described by Johnson *et al* (1968) and Mehta *et al* (1977). For these calculations we used a matching radius  $a_c$  equal to  $1.05 A + 1.5 F$  (Robson 1966). In calculating  $\Gamma_p$  and  $W$  we have made use of the following expressions (Johnson *et al* 1968)

$$\Gamma_p = - \frac{2\Delta P_p^*}{(S_p^* - B_c)}$$

$$\text{and } W = \pi S_p^* \left( \frac{S_p^* - B_c}{P_p^*} \right)^2 P_p^* \Gamma_p \quad (6)$$

where the quantities  $S_p^*$ ,  $B_c$ ,  $P_p^*$ , and  $s_p^*$  have the usual meaning. We used for  $s_p^*$  and  $P_p^*$  for the resonance at  $E_p \approx 1.95$  MeV the values 0.0496 and 0.01 respectively. For the resonance at  $E_p \sim 4$  MeV we used the values 0.0558 and 0.347 for the same quantities. The results of this analysis are given in table 3. The  $\Gamma_p$  and  $W$  values obtained from other works are also tabulated for comparison (table 3). In general, the  $\Gamma_p$  values from the present work agree very well with those determined by other workers. However, there are differences in  $W(\Gamma_n)$  values. For the IAR at  $E_p \sim 1.95$ , Jones *et al* (1966), Wilhelm *et al* (1969), Gaarde *et al* (1972) have determined  $W$  based on an analysis of individual fine structures. However, we determine  $W$  from ana-

lysis of IAR averaged over fine structures. This may account for the differences in  $W$  values obtained from various methods. In both the cases we find  $\Gamma_A > \Gamma_p + W$  and this result is consistent with the observation made by Robson (1969) in the ( $p, n$ ) analysis.

**3.3c Determination of  $S_n$ .** It has been established (Thompson and Ellis 1969; Kailas *et al* 1979) that the neutron spectroscopic factor ( $S_n$ ) determined from IAR analysis is in very good agreement with that extracted from ( $d, p$ ) data on the same target. Utilising the familiar relationship between  $\Gamma_p$  and  $S_n$  (Mehta *et al* 1977), the neutron spectroscopic factor ( $S_n$ ) for the two IARs measured in the present work have been extracted. The computer code SEARCH (van Bree 1975) and the proton and the neutron optical model parameters listed in table 1 have been used in the determination of  $S_n$ . As  $S_n$  varies with the channel radius  $a_c$ , the  $S_n$  values have been determined for  $a_c$  around 6 fm consistent with the value recommended by Robson (1966). The  $S_n$  values are given in table 3. The  $S_n$  value from the present work is smaller compared to that obtained from the stripping data (Kashy *et al* 1964). However, our result is in good agreement with those obtained by Jones *et al* (1966) and Wilhelm *et al* (1969). The  $S_n$  value for the first excited state obtained from the present work is in excellent agreement with those obtained by Kashy *et al* (1964) and Jones *et al* (1966). It is encouraging that  $\Gamma_p$  and hence  $S_n$  can be determined exclusively from our analysis of ( $p, n$ ) data and these  $S_n$  values compare favourably with the ones determined from the stripping data.

#### 3.4 Intermediate width structures

It has been shown by Kailas *et al* (1982) that gross structures which could be due to intermediate reaction mechanism appear in ( $p, n$ ) reaction excitation functions averaged over  $\sim 100$  keV energy intervals. In order to see whether this feature is seen in the present case as well, we have averaged the fine structure excitation function over  $\sim 60$  keV and this is displayed in figure 8. There are several broad structures with widths  $\sim 60$  keV or more but they are not in general prominent, excepting the ones at  $E_p \sim 2, 4$  and 5 MeV. The first two correspond to positions of IARs. We have compared the level spacings of these gross structures with the predictions of Izumo's partial equilibrium model (Izumo 1965). The calculations are for the  $K$  values (quasiparticles) 5 and 6 which are appropriate for  $^{48}\text{Ca} + p$  system. There is excellent agreement between the theory and the experiment (figure 8). We may add that  $\Delta E \sim 60$  keV is a representative value for the averaging interval and the present conclusions are not very sensitive to this  $\Delta E$  value. It is understandable that for  $\Delta E \sim 100$  keV, we will see less number of broad structures and for  $\Delta E \sim 40$  keV, we will observe more number of gross structures.

#### 4. Conclusion

The present investigation involving the study of the ( $p, n$ ) reaction on  $^{48}\text{Ca}$  has resulted in the determination of proton optical model parameters for  $^{48}\text{Ca}$  at sub-Coulomb energies. The depth of the imaginary potential ( $W$ ) determined from the

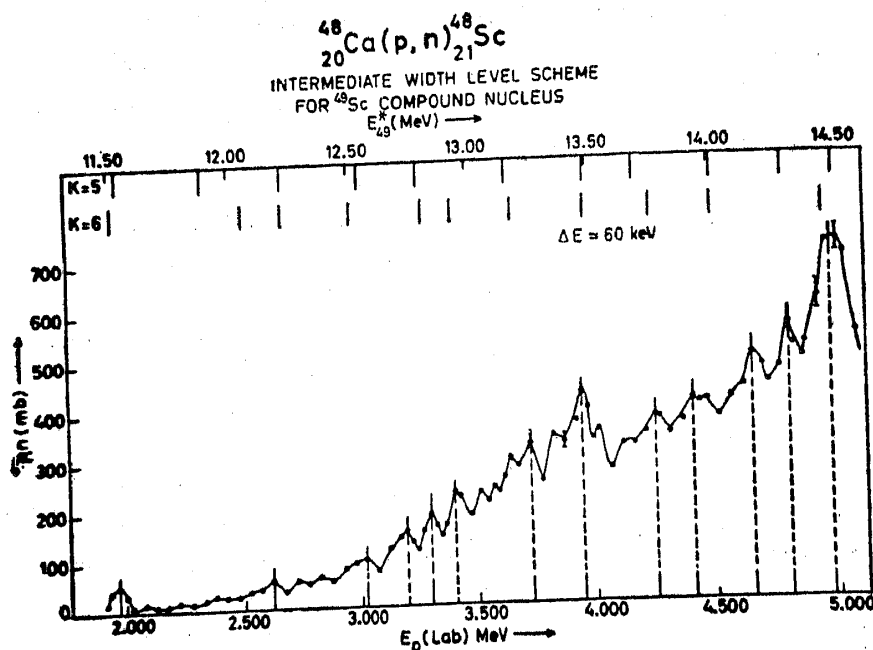


Figure 8. Intermediate width structures (iws) observed in the 60 keV energy-averaged excitation function. The vertical lines (bottom) indicate the positions of iws observed experimentally. The corresponding excitation energies can be obtained from the energy axis on the top of the diagram. The two rows of vertical lines above the excitation function provide the level schemes predicted by the Izumo's partial equilibrium model for two values of  $K$  ( $K = 5, 6$ ), the number of outer nucleons.

present work is smaller when compared to that obtained from a global optical model analysis (Kailas *et al* 1975a) for  $A$  from 45 to 59. This difference may be due to the closed shell nature of the nucleus we have considered here. Detailed fluctuation analysis of the fine structure excitation function has led to a more reliable value for the coherence width  $\langle \Gamma \rangle$ . From a shape analysis of the IARS observed, it has been possible to determine the quantities  $\Gamma_p$  and  $S_n$  and these values compare very well with those obtained from other methods. Further, the level spacings of gross structures seen in this reaction follow nicely the trend predicted by Izumo's partial equilibrium model.

#### Acknowledgements

The help of Mr C V Fernandes and Mr V V Tambwekar at various stages of the experiment is gratefully acknowledged. The cooperation of the van de Graaff staff in the smooth running of the machine is appreciated. One of us (Gs) thanks the Department of Atomic Energy for the award of fellowship.

#### References

- Braga Marcazzan M G and Milazzo Colli L 1970 *Prog. Nucl. Phys.* **11** 145  
 Chilosi G, Ricci R A and Vingiani G B 1968 *Phys. Lett.* **20** 159  
 El Nadi L M *et al* 1965 *Nucl. Phys.* **64** 449  
 Gaarde C, Kemp K, Petresch C and Folkmann F 1972 *Nucl. Phys.* **A184** 241

- Gilbert A and Cameron A G W 1965 *Can. J. Phys.* **43** 1446
- Gove N B and Wapstra A H 1972 *Nucl. Data Tables* **11** 127
- Hauser W and Feshbach H 1952 *Phys. Rev.* **87** 366
- Izumo K 1965 *Nucl. Phys.* **62** 673
- Jänecke J 1969 *Isospin in nuclear physics* (ed.) D H Wilkinson (Amsterdam: North Holland) p. 297
- Johnson C H, Kernell R L and Ramavataram S 1968 *Nucl. Phys.* **A107** 21
- Jones K W *et al* 1966 *Phys. Rev.* **145** 894
- Kailas S, Mehta M K, Viyogi Y P and Ganguly N K 1975a *Nucl. Phys. Solid State Phys. (India)* **B18** 12
- Kailas S *et al* 1975b *Phys. Rev.* **C12** 1789
- Kailas S, Gupta S K and Mehta M K 1976 BARC-I-360
- Kailas S *et al* 1979 *Nucl. Phys.* **A315** 157
- Kailas S, Gupta S K and Mehta M K 1982 (to be published)
- Kashy E, Sperduto A, Enge H A and Buechner W W 1964 *Phys. Rev.* **B135** 865
- McMurray W R *et al* 1967 *Nucl. Phys.* **A99** 17
- Mehta M K, John J, Kerekatte S S and Divatia A S 1966 *Nucl. Phys.* **89** 22
- Mehta M K, Kailas S, and Sekharan K K 1977 *Pramana* **9** 419
- Moldauer P A 1964 *Phys. Rev.* **B135** 642 *Rev. Mod. Phys.* **36** 1079
- Robson D 1966 *Isobaric spin in nuclear physics* (eds.) J D Fox and D Robson (New York: Academic Press) 411
- Robson D 1969 *Isospin in nuclear physics* (ed.) D H Wilkinson (Amsterdam: North Holland) 463
- Sekaran K K and Mehta M K 1969 *Proc. Conf. on Properties of Nucl. States, Montreal University* 763
- Thompson W J and Ellis J L 1969 *Nuclear isospin* (ed.) J D Anderson *et al* (New York: Academic Press) 689
- van Bree R 1975 private communication
- Vingiani G B, Chilosi G and Bruynesteyn W 1968 *Phys. Lett.* **B26** 285
- Viyogi Y P and Ganguly N K 1976 BARC report (unpublished)
- Viyogi Y P *et al* 1978 *Phys. Rev.* **C18** 1178
- Wilhjelm P *et al* 1969 *Phys. Rev.* **177** 1553
- Zyskind J L *et al* 1979 *Nucl. Phys.* **A315** 430